SPE-232849-MS

Unique hardness and porosity patterns in siliceous rocks of the Monterey Formation, Belridge Oil Field, California

R. W. Weller[1], and R. J. Behl[1]
[1]Department of Earth Science, California State University, Long Beach, California, USA

This paper was prepared for presentation at the Pacific Section AAPG/SPE Western Regional Joint Meeting, Bakersfield, CA, USA, 12 - 16 April 2026.

Abstract

We quantify how the proportion of diagenetic silica relative to clay-rich detritus influences hardness in all silica phases in upper Monterey Formation rocks, San Joaquin Basin, California. The rebound hardness and porosity of highly siliceous mudstones evolve during multiple stages of silica diagenesis (opal-A to opal-CT to quartz), influencing reservoir properties and the occurrence of natural and induced fractures. Rocks with higher silica content are harder for all diagenetic silica phases, but the dataset is too limited to evaluate this relationship in opal-A diatomaceous rocks. Hardness increases in clear steps between silica phases: increasing by 69% from opal-A to opal-CT, but only 10% from opal-CT to quartz. Even partial cementation in mixed opal-A/opal-CT rocks produces a dramatic increase in rock strength. A further increase in hardness by 24% occurs with no additional silica-phase change, likely via compaction and cementation associated with illitization and catagenesis in burial to over 12,000'. In the Belridge field, these changes in hardness are connected with reductions in average porosity from about 60% to 40% to 20% to 8% at about 2,000', 5,500', and 12,000' of burial depth, respectively.

A unique and surprising relationship exists between porosity and rock strength for biosiliceous and diagenetic siliceous rocks of each specific silica phase. Sedimentary rocks typically show a strong inverse relationship between rock strength and porosity: as porosity increases, rock strength decreases. However, for each studied set of opal-A, opal-CT, mixed opal-A/CT or quartz phase rocks, hardness increases with porosity! This is likely due to the decreasing abundance of ductile, malleable, and uncemented detrital grains (clay, silt) in increasingly siliceous rocks, while rigid and open frameworks of diagenetic opal-CT or quartz become more interconnected and competent.

Key Words

Hardness, porosity, silica diagenesis, mudstone, shale

Introduction

Understanding rock strength is critical to correctly predicting fracture distribution in unconventional reservoirs (Pitman et al., 2001; Gale et al., 2007), predicting the sealing capacity of caprocks (Ingram and Urai, 1999) and controlling wellbore stability in drilling (Holt et al., 2015). Composition is a fundamental parameter that is well correlated to a wide range of rock strengths and mechanical behaviors in mudstones (Gross, 1995; Britt and Schoeffler, 2009; Crawford et al., 2010; Passey et al. 2010). Particular to siliceous mudstones such as the Monterey Formation, Woodford Formation, and Horn River Group, authigenic quartz has been indicated as a strong and brittle component key to creating dense and communicable fractures, while abundant clay minerals correlate with weak and ductile rocks, inhibiting fracture formation (Ross and Bustin, 2008; Blood et al. 2013; Dong et al., 2017).

The Miocene Monterey Formation of California is highly siliceous, yet complexly heterogeneous in its carbonate, phosphate and organic-matter content (Isaacs, 1980; Behl, 1999). It is nearly unique in that it still preserves strata of all 3 phases of silica: Opal-A (chiefly as diatomaceous sediment), opal-CT (as chert, porcelanite and siliceous mudstone) and quartz (also as chert, porcelanite and siliceous mudstone) (e.g., Bramlette, 1946, Murata and Larson, 1975; Isaacs, 1981a, etc.). The Monterey is the main petroleum source rock in California as well as an important reservoir rock in many oil fields (Isaacs and Petersen, 1987; Reid and McIntyre,2001; Tennyson and Isaacs, 2001; Schwalbach et al., 2009). Its rocks form both matrix-supported (opal-A diatomite and quartz-phase porcelanite) and fractured reservoirs (opal-CT and quartz-phase chert and porcelanite, and dolomite). The wide variety of compositions of Monterey Formation siliceous mudstones makes them excellent analogs for the understanding and interpretation of other unconventional shale plays in which authigenic silica may be a major influence on geomechanical behavior.

This study examines the geomechanical properties of the upper Monterey Formation in the San Joaquin Valley of California by measuring rebound hardness. Compositionally equivalent samples from multiple reservoir lithologies at depths between 800’ to 12,500’ TVD are compared to quantify and distinguish the controls of rock strength in siliceous mudstones. The results apply to reservoirs estimated to hold hundreds of millions to billions of barrels of oil in California (Allan and Lalicata, 2011; Kuuskrra et al., 2013; Larue et al., 2018).

Background

Monterey Formation

The Monterey Formation is a middle- to upper-Miocene succession of predominantly fine-grained siliceous mudstone with distinct facies that independently serve as source, seal, and reservoir rocks for many conventionally-trapped and prolific petroleum resources of Central and Southern California (Behl, 1999; Tennyson and Isaacs, 2001). The Monterey Formation is incredibly heterogeneous in composition, diagenesis, and depth with a maximum thickness of 10,000' at Chico Martinez Creek (Mosher, 2013). The focus of this study is of the siliceous mudstones of the Monterey Formation, which are dominated by biogenic silica and clay-rich detritus (Bramlette, 1946; Pisciotto and Garrison, 1981). Biogenic silica is chiefly sourced from marine diatoms, associated with coastal upwelling and hemipelagic settling (Ingle, 1981). Fine-grained detritus is sourced from terrigenous runoff and includes clay minerals (principally mixed-layer illite-smectite), feldspars, and quartz (Isaacs, 1980; Compton, 1991a). Varieties of highly siliceous mudstone that differ by detrital content or silica phase are given specific names such as diatomaceous mudstone, diatomite, porcelanite or chert in the California and Pacific Rim literature (Bramlette, 1946; Isaacs, 1981a). Not only are silica and fine detritus the two primary components of siliceous mudstones, but they have stark and contrasting effects on the physical and mechanical properties of rocks. Opaline and diagenetic silica create a framework of interlocking biogenic to crystalline components with higher porosity and rock strength as well as increasing the propensity for burial diagenesis and brittle open-mode failure. Conversely, detritus creates a weaker framework of lower porosity and lower strength that in some cases inhibits diagenesis and typically promotes shear failure (Isaacs, 1981ab; Gross, 1995). Thus, describing Monterey Formation mudstones in terms of a silica-to-detritus ratio offers a quick and rough characterization of its physical and mechanical properties. Carbonate, organic matter, and authigenic phosphate are minor components in the distinctly siliceous intervals of the upper Monterey Formation and thus excluded from a bimodal descriptor of silica and detritus.

Silica Diagenesis and Phases

Biogenic silica is geologically unstable and undergoes a two-step diagenetic transformation driven by time and temperature with kinetics modified by sediment composition (Fig. 1a). With burial to ~40-50°C, biogenic opal-A (diatomite) silica undergoes an *in situ* dissolution and precipitation into metastable opal-CT. A similar reaction occurs again at ~65-80°C when Opal-CT undergoes an *in situ* dissolution and then precipitation as diagenetic quartz (Pisciotto, 1981; Keller and Isaacs, 1985). The range of alteration temperature are primarily related to the presence of smectite clays, which retard the opal-A to opal-CT transformation but accelerate the opal-CT to quartz-phase transformation (Murata and Larson, 1975; Isaacs, 1981b).

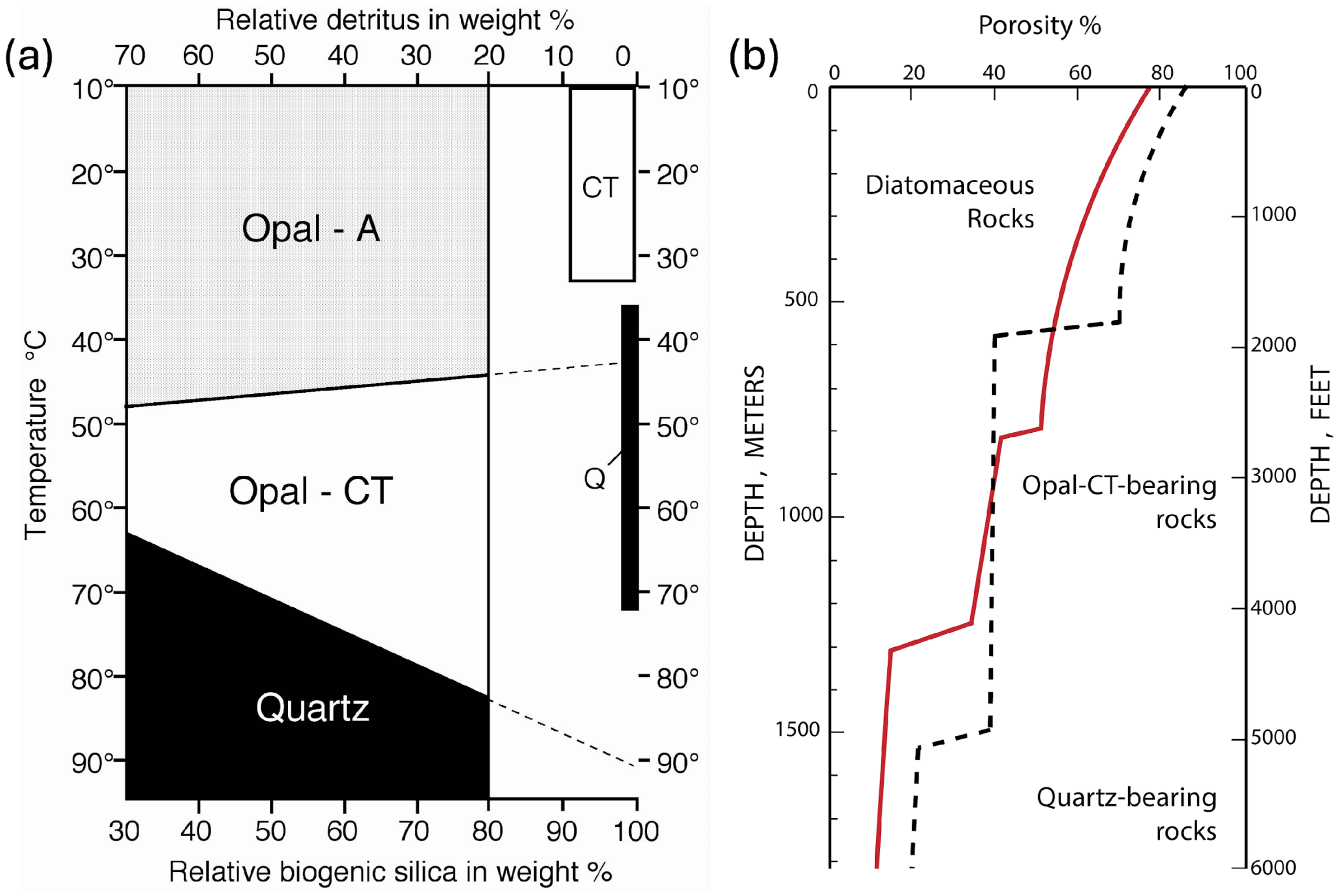

Fig. 1—Schematic diagrams of silica diagenesis. (a) Three-phase silica diagenesis with regard to temperature and compositional controls based on studies of the California coast. Note that cherts (right side of chart) can form at much lower temperatures than opal-CT porcelanite and siliceous mudstone (Keller and Isaacs, 1985; Behl and Garrison, 1994). (b) Porosity reduction in siliceous mudstones of the Monterey Formation through physical and chemical compaction. The solid red line represents detritus-rich siliceous rocks and altering from opal-A to opal-CT at greater depths and compacting more within each phase, the dashed line represents low-detritus siliceous rocks with greater porosity and greater resistance to compaction (modified from Isaacs et al., 1983).

Silica diagenesis reduces porosity and thus volume in stepwise shifts of physical and chemical compaction, resulting in dramatic alteration to mechanical rock properties (Figure 1b; Isaacs, 1981b; Compton 1991b). Porosity loss changes permeability and physical strength by altering pore geometry, effective pore connectivity, and grain-to-grain contacts creating a denser rock volume (Isaacs, 1980; Schwabach et al., 2009; Kassa, 2016, Behl and Kassa, 2026, in press). Rocks of greater diagenetic silica content have more matrix dispersed diagenetic silica – either cryptocrystalline opal-CT or microcrystalline quartz – and a strong crystalline framework with higher strength and higher brittleness (Isaacs, 1981a; Snyder et al., 1983; Gross, 1995). Highly siliceous opal-CT and quartz-phase lithotypes resist burial compaction while detritus-rich lithotypes experience greater compaction via grain rotation, crushing, and deformation (Isaacs, 1981b). Monterey Formation lithologies are classified by both their bulk composition and diagenetic phase with associated properties relevant to their porosity and fracture potential.

Mechanical Behavior and Rock Composition

It is widely documented that the Monterey Formation has a diverse expression of physical properties and mechanical behaviors related to primary composition (silica and detritus) and silica diagenesis (Bramlette, 1946; Isaacs, 1981b; Snyder et al., 1983; Gross, 1995; Wirtz and Behl, 2022). In general, rocks of any silica phase with greater percentages of clay-rich detritus are easier to scratch, less cohesive, and prone to faulting rather than jointing, while greater amounts of diagenetic silica have the opposite influence on nearly every physical or mechanical property (Isaacs, 1981a; Snyder et al., 1983). Chert is different than the bulk of other siliceous lithologies and has an exceptionally high hardness, low porosity, and distinct vitreous texture (Isaacs, 1981a; Snyder et al., 1983; Behl and Garrison, 1994). The different impact of opal-CT and quartz-phase diagenetic silica on mechanical properties of overwise similar composition (e.g., silica: clay ratio) has not been quantified (Isaacs, 1981a). Additionally, no published studies have reported on the alteration of quartz-phase mudstones at depth of greater than 10,000'.

Previous Hardness Studies

Rebound hardness (HLD), a ratio of a probe's impact velocity divided by the rebound velocity as defined by Leeb (1979), has been demonstrated to be a fast, non-destructive, and effective tool for estimating unconfined compressive strength (UCS) at less than a 1 cm^2 resolution (Verwall and Mulder, 1993; Aoki and Matsukura, 2008; Lee et al., 2014). Rebound hardness is not the same as Mohs (1825) mineralogical hardness, although there is a weak positive exponential relationship (Broz et al., 2006). Several studies have demonstrated a strong correlation of rebound hardness to sonic velocity and/or fracture style due to lithological variation in core and outcrop (Ritz et al., 2014; Rolfs, 2015; Murray, 2015; Offurum, 2016; Becerra-Rondon, 2017; Dong et al., 2017).

Study Location

The Belridge oil field is located in the southwestern San Joaquin Basin approximately 45 miles NW of Bakersfield, 55 miles SE of Coalinga, and 5 miles east of Chico Martinez Creek in Kern County, California (Figure 2a). The Belridge oil field is an elongated *en echelon* anticlinal structure in the western San Joaquin Basin (Graham and Williams, 1985; Mount and Suppe, 1987). Monterey Formation reservoirs in the Belridge oil field have produced over 300 MMBO with a long history of primary and secondary recovery techniques used to produce 25-39° API oil from low-permeability rocks including various fracture techniques (Allan and Lalicata, 2012). Monterey Formation members examined in this study of the Belridge oil field include the Reef Ridge (locally the Belridge Diatomite) and the McClure Shale (locally divided as the Antelopes Shale and McDonald Shale) (Graham and Williams, 1985; Schwartz, 1988; Bowersox, 1990; Miller and McPherson, 1992; Allan and Lalicata, 2012). Highly siliceous mudstones of the Monterey Formation in the Belridge oil field have thin to thick beds of variable silica:detritus ratios and are buried at different depths (400' – 14,000') along the flanks of the anticline (Fig. 2b) where physical and diagenetic contrasts develop within laterally continuous strata. The opal-A-phase Belridge Diatomite is predominately located at less than 2,000' TVD along the crest of the anticline, with opal-CT phase Belridge Diatomite (aka "brown shale") or the Antelope Shale encountered below those depths to a maximum of 5,800’ (Schwartz, 1988; Bowersox, 1990). Along the flanks of the anticline, the Antelope-McDonald stratigraphic horizon plunges from approx. 6,100’ to greater than 12,500’.

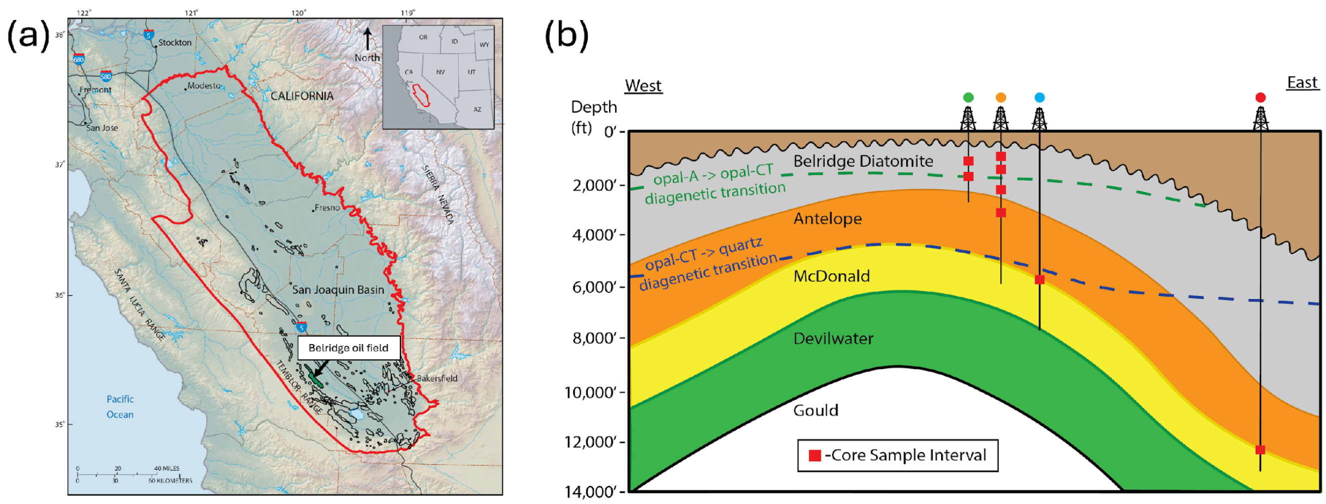

Fig. 2—Location map. (a) Belridge oil field (green) in the south-west of the San Joaquin Basin (red outline), Kern County, California. Other San Joaquin oil fields are outlined in black. Modified from USGS PP 1713, Hosford Schierer (2007); (b) Schematic of the Belridge oil field and cored intervals in this study. Note the differences in diagenetic horizons (dashed) that cut lithostratigraphic members.

Methods

Core, core data, and wireline logs were studied from four wells in the Belridge oil field area. Compositionally and diagenetically diverse intervals were targeted at stratigraphically similar horizons to test an extensive range of siliceous Monterey Formation rocks from the crest, shoulder, and plunging flanks of the Belridge Anticline (Fig. 2b). We used well logs (gamma ray, density, neutron-porosity, and sonic velocity), core photos, and core data evaluating composition, porosity, and oil saturation, as well as observations of bedding and texture to select a range of core samples that represent the range of lithofacies for analysis. Core samples are from both silica-rich and clay-rich beds from similar stratigraphic intervals in multiple wells. Thinly bedded, laminated, massive, and gradational bedding fabrics are represented. See Weller (2018) for detailed explanation of petrophysical criteria, and methods of surface preparation, X-ray Fluorescence (XRF) scanning, X-ray Diffraction (XRD), compositional calibration and hardness testing. The diagenetic phase of silica (opal-A, opal-CT, quartz) was determined from XRD analyses and confirmed by petrographic observations of microfossil preservation.

A total of 28 ~3’-long core sections were used for this study (Table 1). Five sample groups (opal-A, mixed-A+CT, opal-CT, 6k’-quartz, and 12k’-quartz) were defined by silica phase and/or burial depth. Core intervals with volcanic ash, carbonate, abundant fractures, or extreme fissility were initially included in measurements, but later excluded to focus on variations in the properties of siliceous mudstones while minimizing complicating variables. Although rejecting highly fractured intervals may have excluded data from some of the most brittle rock types, the wide range and large number of accepted measurements likely incorporated these end-member lithotypes, nonetheless. A Proceq Equotip Piccolo 2 tester with a type-D impact tip was used to measure Leeb-hardness type-D (HLD) values. Hardness testing was taken at the same location and spatial resolution as XRF data by using a scale from line scan images recorded on the Avatech XRF scanner. Normalized composition of percent silica (biogenic or diagenetic) and detritus (aluminosilicates and detrital quartz) are calculated from % oxides of SiO_2 and Al_2O_3 using Isaacs's (1980) equations developed for the Monterey Formation. These equations were developed in the Santa Barbara coastal area and likely slightly underestimate silica and slightly overestimate detritus in the San Joaquin Basin.

Table 1— Summary of cores from each sample group in this study.

Sample Group Name	Depths (TVD)	Member	Silica Phase	Ave HLD points tested	Field Location	Year Drilled	Porosity (%)
Opal-A	800' – 1,370'	Belridge Diatomite	opal-A	454	North and South Belridge	2000	59 – 67
Mixed-A+CT	1,900' – 1,930'	Belridge Diatomite & Antelope Shale	13% opal-A 87% opal-CT	118	South Belridge	2000	46 – 55
Opal-CT	2,200' – 3475'	Belridge Diatomite & Antelope Shale	opal-CT	313	North Belridge	2000	33 – 56
6k'-quartz	6,100' – 6,150'	lower Antelope & upper McDonald	quartz	189	SE North Belridge	2013	12 – 27
12k'-quartz	12,500' – 12,577'	lower Antelope & upper McDonald	quartz	415	East of Belridge (Buttonwillow)	2012	2 – 7

Results

Well-Log Petrophysics

In the study area, opal-A intervals typically exhibit the highest porosity (average 63% DPHI) (verified by an average core plug porosity of 62.5%) and lowest bulk density (RHOB). In the 7122A-2 and 548D1-35N wells, the opal-A to opal-CT transition zone is identified by an initial rapid shift from 55% porosity to less than 49% porosity over a 185' to 200' thick interval, followed by a 315' to 400' section with a slower rate of porosity reduction to < 46%. The bulk opal-CT interval has a consistent and stable log character with minor lithological variance within the brown shale subdivision. The opal-CT to quartz phase transition zone is approximately 420' thick with an 18% to 20% reduction in porosity and a 30 µs/ft decrease in sonic velocity. Quartz-phase lithologies (at 6000' - 9500' TVD) have a 10% to 15% DPHI and 2.3 g/cm^3 bulk density. An anomalous step in reduced porosity, increased density, and increased sonic velocity occurs between 9,640' and 10,950' entirely within the quartz-phase zone. The 12k'-quartz phase intervals of the Antelope Shale and McDonald Shale have the lowest porosity (<8% DPHI) and the fastest sonic velocities (70-80 µs /ft) measured.

Composition

Monterey Formation rocks in the Belridge oil field are compositionally heterogeneous and capture a wide range of siliceous composition as indicated by XRF counts normalized to biogenic and diagenetic silica weight percentages. Opal-A and mixed-A+CT sample groups are primarily from the Belridge Diatomite Member and have a lower mean silica percentage of about 35% and range from 15-50% biogenic and diagenetic silica, whereas opal-CT and both quartz-phase sample groups (Antelope Shale Member) have higher mean silica percentages of about 49% and range from 35-70% diagenetic silica.

Matrix Porosity

A distinct and narrow range of both core plug and wireline-calculated porosity is associated with each diagenetic stage or burial group. Opal-A samples have the highest porosity and 12k'-quartz samples have the lowest porosity (Fig. 3). Porosity loss from silica diagenesis is seen in the step from opal-A to opal-CT and then opal-CT to 6k'-quartz. Within each group except the 12k'-quartz group, porosity variation follows a positive linear trend relative to percent biogenic and diagenetic silica (Fig. 3). High silica-detritus ratio opal-CT samples have the highest porosity while lower silica samples have up to 22 percent lower porosity. The porosity of the 12k' quartz group is exceptionally low with little variation across the entire range of silica-detritus ratios.

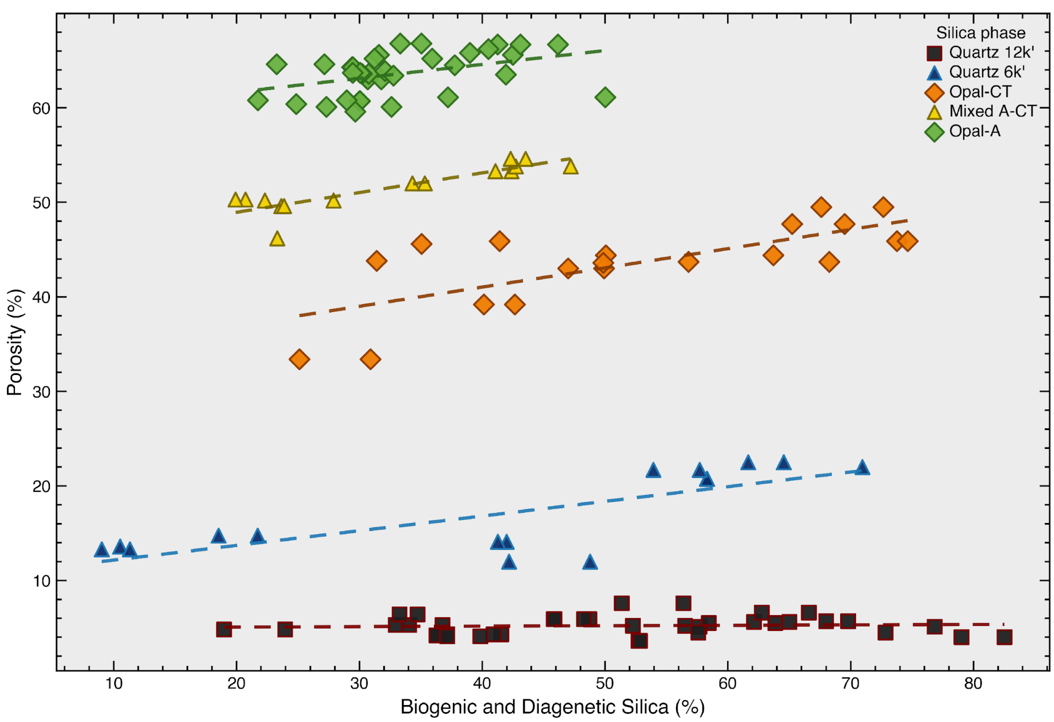

Fig. 3— Core plug porosity in each sample group with dashed log trend correlating composition and porosity. Note the flattened trend and <8% porosity across all percentages of silica in 12k'-Quartz rocks.

Hardness

Monterey Formation siliceous mudstones increase in hardness with each increasing step of diagenesis. Each successive phase also has a distinct range of hardness relative to composition (Fig. 4). Hardness and silica-detritus ratios have a positive linear association in every sample set except for the limited compositional-range dataset for opal-A (Fig. 4; Table 2). Since no high-silica samples were available from the opal-A cores, three outcrop samples with >70% biogenic silica composition were measured for approximate comparison. Samples have rebound hardness values ranging from 400 to 480 HLD, suggesting a higher HLD in clean and dry diatomite. Mixed opal-A+CT samples increase on a scale and trend similar to opal-CT. Opal-CT samples have the largest range of hardness values (370 HLD) and greatest rate of change relative to silica and detritus (Fig. 4). Hardness in 6k'-quartz samples is considerably scattered. HLD is 20% greater in 12k'-quartz samples than 6k'-quartz phase samples and is the highest for any compositional range (maximum 872 HLD).

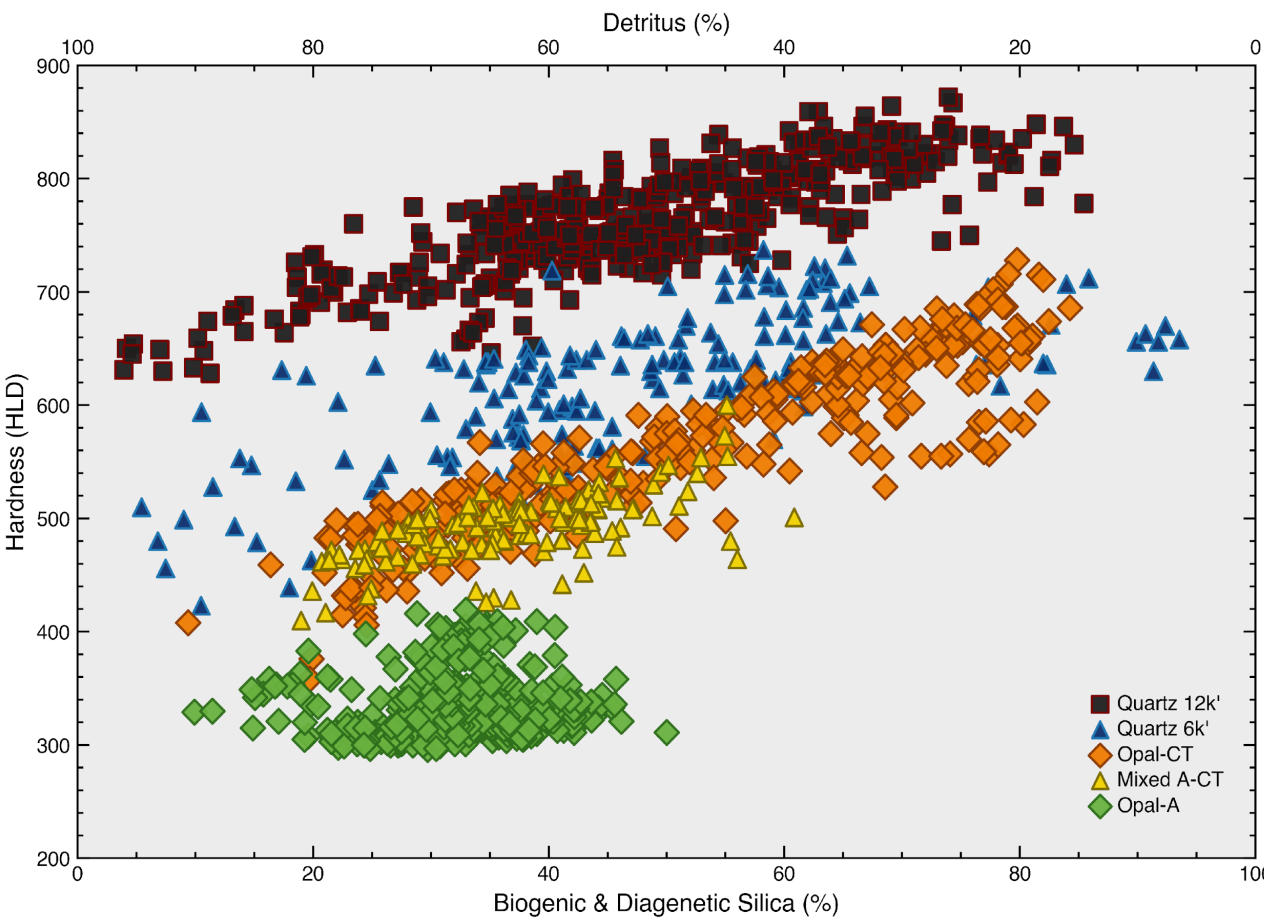

Fig. 4— Data for >2000 average points in five burial groups relative to hardness (HLD) and silica and detritus derived from high-resolution XRF scanning. The hardness of each burial group progressively increases and follows a compositional trend associated with its group. Opal-A samples with greater than 50% silica were not encountered in the cores analyzed.

Table 2— Summary of hardness data.

Silica Phase	Mean Sample Depth	Mean % Silica Biogenic or Diagenetic	Mean HLD of 50-60% silica	Min HLD	Max HLD	HLD Range
opal-A	1,207’	33.9	334	296	410	124
mixed A+CT	1,924’	39.8	505	410	600	191
opal-CT	3,176’	49.9	534	357	728	371
6k’-quartz	6,124’	54.7	603	423	737	314
12k’-quartz	12,526’	50	755	628	872	244

Discussion

Rock Composition and Hardness in Siliceous Sedimentary Rocks

This high-spatial-resolution investigation of the hardness of siliceous mudstones in the Monterey Formation allows quantification and consideration of reservoir heterogeneity at a scale commonly seen in core and outcrop, but difficult to characterize with wireline or core plug data. A key assumption is that hardness is well correlated to other geomechanical characterizations such as sonic velocity, brittleness, and unconfined compressive strength (Murray, 2015; Yang et al., 2015, Aoki and Matsukara, 2008; Lee et al., 2014; Lee, 2015). Low hardness lithologies are most likely to deform ductility, to inhibit fracture propagation, and/or to lead to proppant embedment (Sonnenfeld et al., 2015). These implications are most significant where low and high hardness lithologies are interbedded, influencing the style and timing of fractures in a mechanically stratified succession.

The siliceous mudstones of the Monterey Formation have a tremendous variance in hardness at any stage of burial (Fig. 4). Our data show that rebound hardness is related to composition, diagenesis, and burial history. Composition is the primary control of hardness within any burial group of siliceous mudstones of the Monterey Formation (Fig. 5). There is a strong positive correlation between diagenetic silica and hardness in opal-CT and 12k’-quartz (both R^2=0.97), with only a slightly weaker positive correlation in 6’k-quartz (R^2=0.83). These findings are consistent with other studies on hardness (Ritz et al., 2014; Dong et al., 2017; Becerra-Rondon, 2018). Additionally, our results parallel the compositional relationship to natural fractures styles (Gross, 1995; Lorenz et al., 2002; Gale et al., 2014), unconfined compressive strength (Zoback, 2010), and Young’s Modulus (Kumar et al., 2012) documented from mudstone studies of many other formations. The physical and chemical transformation of silica by burial diagenesis dramatically hardens rocks in two steps although each step of silica diagenesis has a unique hardening effect (Fig. 4). On average, hardening of siliceous mudstones by silica diagenesis is greater from opal-A to opal-CT (average 228 HLD or +68%) than from opal-CT to quartz-phase (average 56 HLD or +10%). Even at a low weight percentage (about 10-15%), diagenetic silica exists as a stiff and hard crystalline matrix component, having the ability to effectively bind and bridge non-silica components. Yet, hardening by silica reaches an effective maximum at 70% silica for quartz-phase rocks and does not increase further with greater silica content (Fig. 4). We find that highly siliceous opal-CT and quartz phase porcelanites of greater than 70% diagenetic silica have a very similar mean hardness of about 675 HLD (Fig. 5). However, data show that quartz-phase mudstones with less silica - or greater detritus – are 9 to 32% harder than opal-CT mudstones.

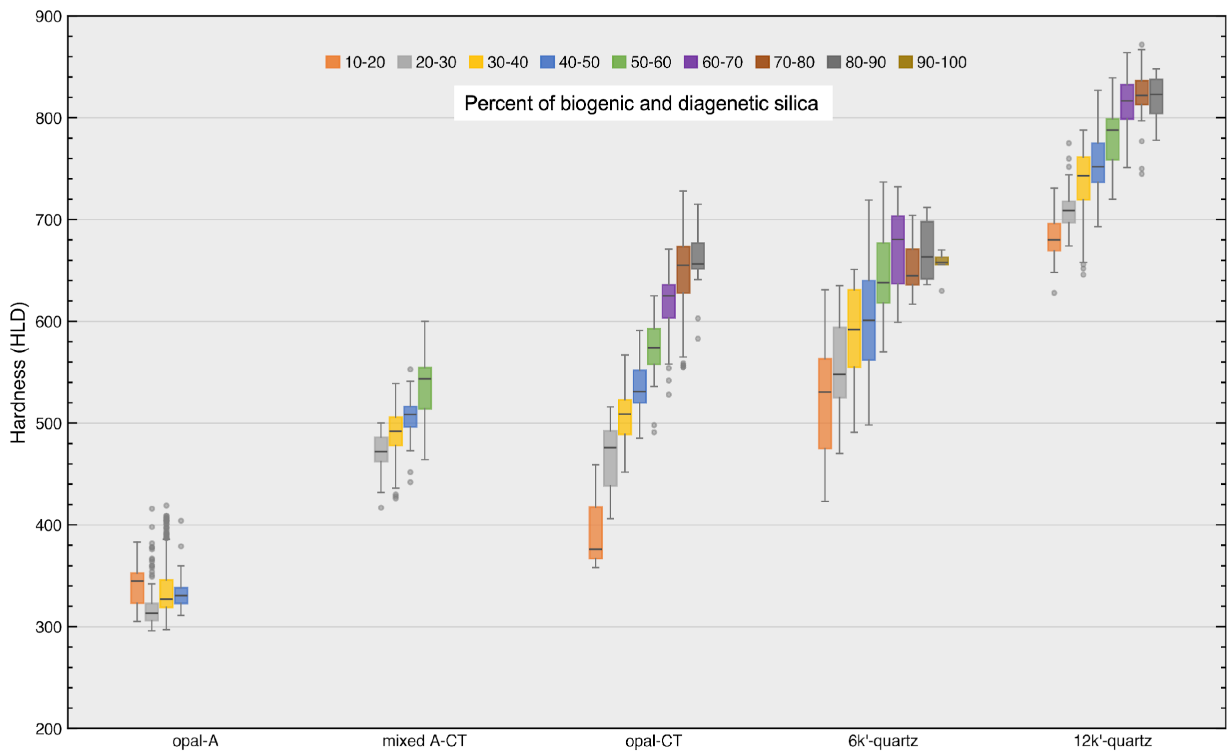

Fig. 5— Quartile box-and-whisker plot of silica classes in 10% steps demonstrates the hardness increases of high-silica vs. low-silica rocks with burial. High-silica opal-CT and 6k' quartz phase rocks have very similar hardness properties. Mixed A-CT samples have a 13:87 A/CT ratio.

Comparison of Monterey Siliceous Rocks with Other North American Shales

Opal-A Rocks

Opal-A diatomaceous rocks in the Monterey Formation have lower mean hardness values than opal-CT or quartz lithotypes. Opal-A diatomaceous rocks in the Monterey Formation have lower mean hardness values than opal CT or quartz lithotypes. Diatomaceous mudstones of the upper Monterey Formation have a porosity of 55-70%, a maximum burial depth of ~2,000 ft, and an age of 5.5 – 6.5 Ma. Opal-A rocks are known to be fracture barriers when juxtaposed against much harder opal-CT rocks (Gross, 1995; Lockman, 2012). While the porosity, age, and depth of Opal-A Monterey Formation rocks are far different from the clay-rich lithotypes of the Horn River and Marcellus shales, both have similar hardness values and the potential to create high contrasts in mechanical stratigraphy.

Opal-CT Rocks

Opal-CT lithologies have a range of hardness (about 370 HLD) and a potential mechanical heterogeneity similar to many other shales. Opal-CT samples of >70% silica have a hardness of about 650-725 HLD, which is equal to or greater than the most silica-rich or carbonate-rich intervals of the Marcellus Formation, Niobrara Formation, Eagle Ford, or Austin Chalk, all of which are known - and relied upon - to strain with brittle fractures at greater depths. Notably, lower hardness opal-CT lithologies of 370-515 HLD are similar to the marls of the Niobrara and Eagle Ford, or clay-rich intervals of the Marcellus and Woodford shales. Each of these lower hardness shales have been shown to exhibit shear failure, fracture inhibition, and low fracture intensity (Murray, 2015; Ritz et al., 2014; Offurum, 2016; Becerra-Rondon, 2018)

6'k-Quartz Rocks

Quartz-phase rocks of the upper Monterey Formation are as hard as, or typically harder than, most other more deeply buried shales. Highly siliceous intervals of the 6k'-quartz section are harder than any of the highly calcareous lithotypes of the Niobrara, Eagle Ford, or Austin Chalk (Ritz, 2014; Murray, 2015). In the Monterey Formation, diagenetic or authigenic quartz is very effective at hardening. Just 15% diagenetic quartz in 6k'-quartz samples creates a higher minimum and median hardness lithology than detrital-rich and more deeply buried intervals of the Marcellus, Horn River, and Eagle Ford shales.

12'k-Quartz Rocks

12k'-quartz-phase lithologies of the upper Monterey Formation are some of the most consistently hard successions of fine-grained mudstones known to exist from this formation. The least hard and most detritus-rich 12k'-quartz samples from the Monterey Formation are frequently as hard or harder than the bulk of Niobrara, Eagle Ford, Austin Chalk, Bakken, and Woodford Shale lithotypes. 12k'-quartz lithologies with >40% silica are also harder than most of the measured siliceous intervals of the Marcellus Formation and equal to or greater than most of the Horn River Formation. Overall, 12k'-quartz lithologies with greater than 70% silica are immensely hard, with a mean 820 HLD that is only comparable to Woodford Shale chert.

The Relationship of Rock Strength or Hardness to Porosity

There is fundamentally an inverse relationship between porosity and rock strength in sedimentary rocks, as an increase in pore volume reduces the load-bearing mineral framework and decreases the surface area of grain-to-grain contacts (Fig. 6; Aoki and Matsukura 2008.; Benavente et al. 2021; Desarnaud et al. 2019; Güneş Yilmaz and Göktan 2018; and Peng et al. 2020). This relationship is largely derived from sandstone and limestone (Vernik et al., 1993, Farquhar et al., 1994; Palchik, 1999; Palchik and Hatzor 2004), mudstones with less than <15% porosity (Lashkaripour, 2002), mudstones with moldic porosity (Zahm and Elderlin, 2010), or unconsolidated Tertiary or younger shales (Horsrud, 2001; Chang et al., 2006). This has been shown by both empirical and theoretical modeling studies (e.g., Xiao et al. 2025). Consequently, modern predictive models often integrate porosity with other textural parameters like grain size and cementation to accurately estimate the Unconfined Compressive Strength of weak sedimentary formations (Atapour and Mortazavi, 2018).

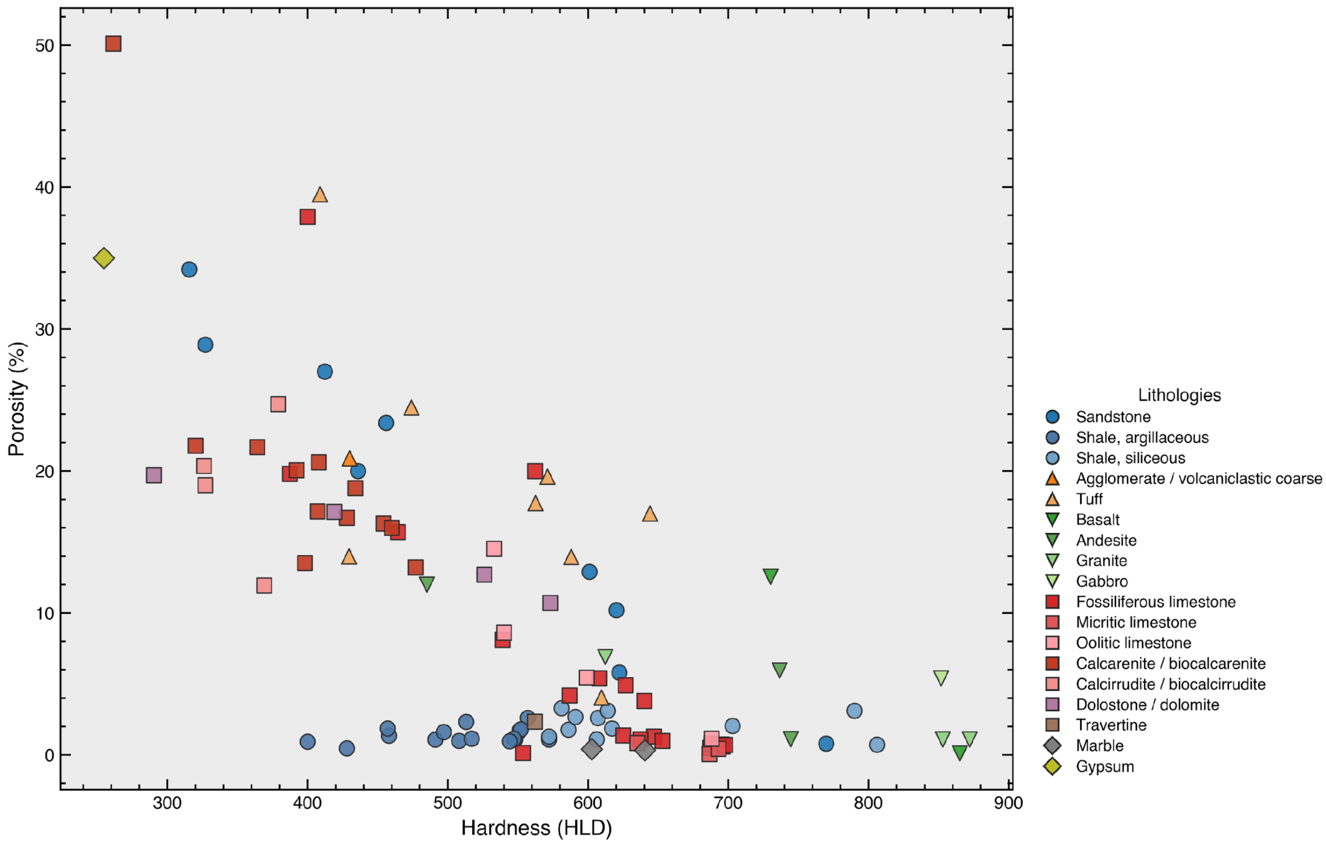

Fig. 6— The general relationship between percent porosity and hardness (HLD) in rocks. Compiled from Aoki and Matsukura 2008.; Benavente et al. 2021; Desarnaud et al. 2019; Güneş Yilmaz and Göktan 2018; and Peng et al. 2020

In contrast, the biosiliceous and diagenetic rocks of the Monterey Formation display a unique and surprising relationship between porosity and rock strength. When including all silica phases and burial depths (opal-A to mixed-opal-A/CT to opal-CT to 6'k quartz to 12'k quartz), core plug porosity has a negative correlation with hardness (Fig. 7), but within each burial group from opal-A through 6k'-quartz phase rocks, there is a positive relationship between porosity and hardness (Fig. 7). Although mean HLD increases with phase change, each step is less than the variability within any one silica phase group (Fig. 5). The positive relationship between porosity and hardness is likely due to the decreasing abundance of ductile, malleable, and uncemented detrital grains (clay, silt) in increasingly siliceous rocks, while rigid and open frameworks of diagenetic opal-CT or quartz become more interconnected and competent. (Isaacs, 1981b). Connected silica crystallites (opal-CT or quartz) are not free to reorient and compact as detrital grains do in highly porous sandstones. Consequently, silica-rich, detritus-poor lithologies maintain porosity through burial and only decrease in porosity and increase in hardness at diagenetic steps.

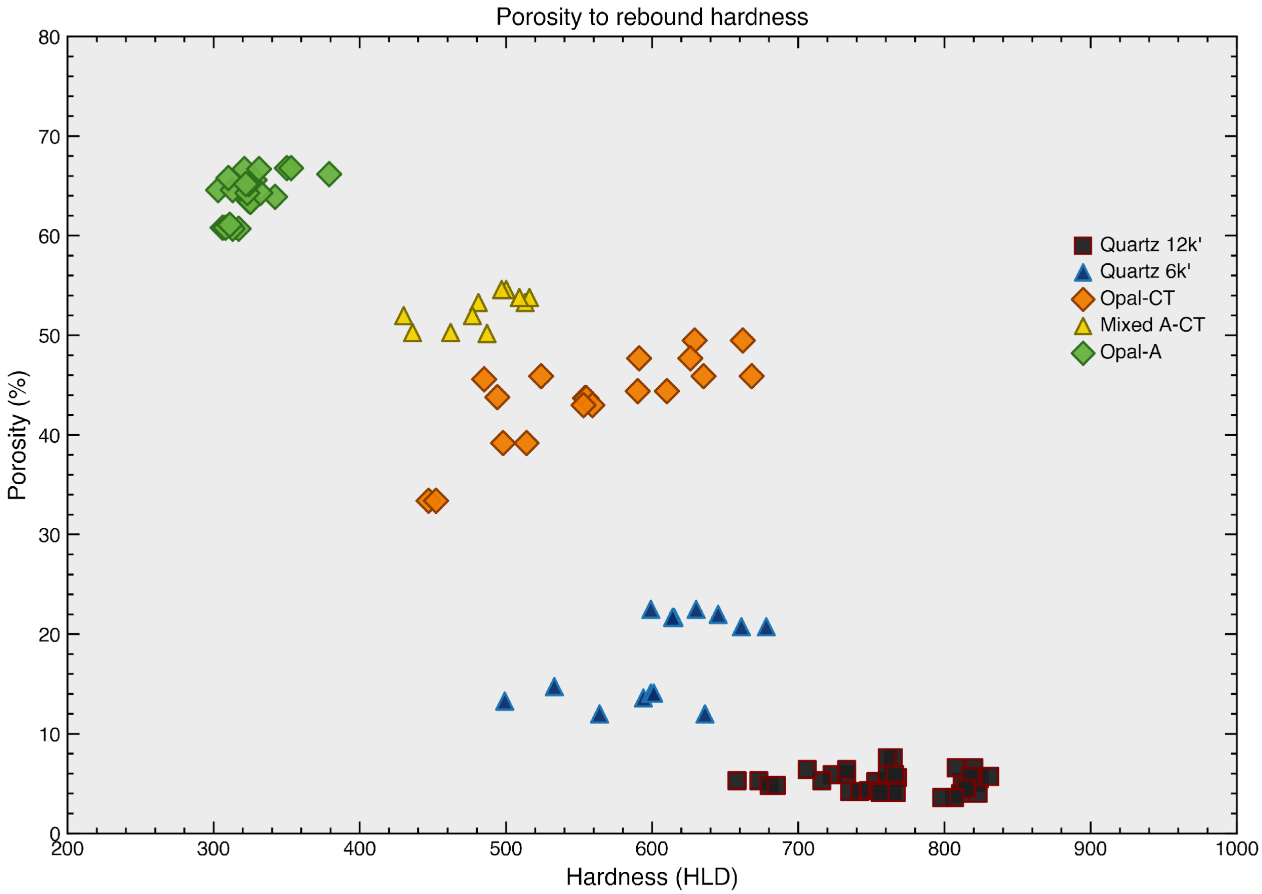

Fig. 7— The relationship between percent porosity and hardness (HLD) in siliceous sedimentary rocks. Across all silica phases and burial depths, core plug porosity has a negative correlation with hardness, but within each burial group from opal-A through 6k'-quartz phase rocks, there is a positive relationship between porosity and hardness. Note the flattened trend in 12k'-Quartz rocks where a low and narrow range of porosity is non-correlative to the wide variability in hardness.

Conclusions

This study quantified the hardness of siliceous mudstones of varied diagenetic stages and burial depths. X-ray florescence scanning (XRF) and micro-rebound hardness (HLD) measurements show that the hardness of siliceous mudstones increase and evolve through two major steps of silica diagenesis. A third increase in hardness at greater than 10,000' of burial depth is less understood but likely related to clay diagenesis, kerogen catagenesis, and physical compaction. The main findings are:

1. Composition (defined by silica:detritus ratios) is a 1st-order control of rock hardness within any burial group. Argillaceous components have a strong negative correlation with hardness values. Diagenetic silica has a strong positive correlation with hardness. Hardness variability due to compositional variability is greater within each burial group than hardness variation is between stages of silica diagenesis.

2. Hardening by silica diagenesis in silica-rich rocks is greatest at the opal-A to opal-CT (+47.3% HLD) transition and much less at the opal-CT to quartz-phase transition (+4.5% HLD). At the opal-CT to quartz-phase transition, greater hardening occurs through clay compaction and greater grain connectivity in detritus-rich lithologies (+17.5% HLD).

3. Porosity is not a reliable indicator of hardness in siliceous mudrocks. Although hardness increases and porosity decrease with steps of silica diagenesis, within each silica phase, porosity has a negative correlation with detrital content and thus a positive correlation with hardness. These findings are contrary to other studies that find a continuous negative correlation of porosity and rock strength.

4. Opal-CT rebound hardness had the best fit correlation and greatest rate of change in hardness with compositional variation. Opal-CT hardness does not increase with burial and resists mechanical alteration by burial compaction.

5. Quartz-phase rocks at >12,000' of burial depth undergo a 25-30% increase in hardness from 6k'-quartz rocks without further silica phase change. We propose that clay diagenesis and early oil catagenesis accelerates burial compaction and hardening. Additionally, silica cementation released by the illite-to-smectite transformation may also play a role in porosity reduction and the increase of hardness.

Acknowledgements

This research was financially supported by the affiliate companies of the CSULB MARS Project (Monterey and Related Sediments) without restriction. Aera Energy LLC and California Resources Corporation graciously supplied core, data, and equipment in support of this study.

References

Allan, M. E. and Lalicata, J. J. 2011. The Belridge giant oil field—100 years of history and a look to a bright future. Presented at the AAPG International Conference and Exhibition, Milan, Italy, 23–77.

Aoki, H. and Matsukura, Y. 2008. Estimating the unconfined compressive strength of intact rocks from Equotip hardness. Bulletin of Engineering Geology and the Environment 67: 23–29. https://doi.org/10.1007/s10064-007-0116-z.

Atapour, H. and Mortazavi, A. 2018. The effect of grain size and cement content on index properties of weakly solidified artificial sandstones. Journal of Geophysics and Engineering 15: 613–619. https://doi.org/10.1088/1742-2140/aaa14a.

Becerra, D., Galvis, H., and Slatt, R. 2018. Characterizing the two principal rock types comprising the Woodford Shale resource play: Application to shale geomechanics. Interpretation 6 (1): SC67–SC84. https://doi.org/10.1190/INT-2017-0146.1

Behl, R. J. 1999. Since Bramlette (1946): The Miocene Monterey Formation of California revisited. In Classic Cordilleran Concepts: A View from California, Geological Society of America Special Paper 338, 301–313. https://doi.org/10.1130/0-8137-2338-8.301.

Behl, R. J. and Kassa, T. G. 2026. Diagenetic evolution of porosity microfabric in biosiliceous sediments, Monterey Formation, California, USA. Frontiers in Earth Science: Sedimentology, Stratigraphy and Diagenesis (in press).

Benavente, D., Fort, R., and Gomez-Heras, M. 2021. Improving uniaxial compressive strength estimation of carbonate sedimentary rocks by combining minimally invasive and non-destructive techniques. International Journal of Rock Mechanics and Mining Sciences 147: 104915. https://doi.org/10.1016/j.ijrmms.2021.104915.

Blood, D. R., Lash, G. G., and Bridges, L. C. 2013. Biogenic silica in the Devonian shale succession of the Appalachian Basin, USA. AAPG Search and Discovery Article 50864.

Bowersox, J. R. 1990. Geology of the Belridge diatomite, northern South Belridge field, Kern County, California. In Structure, Stratigraphy and Hydrocarbon Occurrences of the San Joaquin Basin, California, ed. J. G. Kuespert and S. A. Reid, 215–223. Los Angeles, California, USA: AAPG Pacific Section. https://doi.org/10.32375/1990-GB65.18.

Bramlette, M. N. 1946. The Monterey Formation of California and the origin of its siliceous rocks. US Geological Survey Professional Paper 212 (57 pp.).

Britt, L. K. and Schoeffler, J. 2009. The geomechanics of a shale play: What makes a shale prospective. Paper SPE-125525 presented at the SPE Eastern Regional Meeting, Charleston, West Virginia, USA. https://doi.org/10.2118/125525-MS

Broz, M. E., Cook, R. F., and Whitney, D. L. 2006. Microhardness, toughness, and modulus of Mohs scale minerals. American Mineralogist 91: 135–142. https://doi.org/10.2138/am.2006.1844.

Chang, C., Zoback, M. D., and Khaksar, A. 2006. Empirical relations between rock strength and physical properties in sedimentary rocks. Journal of Petroleum Science and Engineering 51: 223–237. https://doi.org/10.1016/j.petrol.2006.01.003.

Compton, J. S. 1991a. Origin and diagenesis of clay minerals in the Monterey Formation, Santa Maria Basin area, California. Clays and Clay Minerals 39: 449–466.

Compton, J. S. 1991b. Porosity reduction and burial history of siliceous rocks from the Monterey and Sisquoc Formations, Point Pedernales area, California. Geological Society of America Bulletin 103: 625–636. https://doi.org/10.1130/0016-7606(1991)103<0625:PRABHO>2.3.CO;2.

Crawford, B. R., Gaillot, P. J., and Alramahi, B. 2010. Petrophysical methodology for predicting compressive strength in siliciclastic "sandstone-to-shale" rocks. Paper ARMA-10-196 presented at the 44th US Rock Mechanics Symposium and 5th US-Canada Rock Mechanics Symposium, Salt Lake City, Utah, USA.

Desarnaud, J., Kiriyama, K., Bicer Simsir, B. et al. 2019. A laboratory study of Equotip surface hardness measurements on a range of sandstones: What influences the values and what do they mean? Earth Surface Processes and Landforms 44 (7): 1419–1429. https://doi.org/10.1002/esp.4584.

Dong, T., Harris, N. B., Ayranci, K., and Yang, S. 2017. The impact of rock composition on geomechanical properties of a shale formation: Middle and Upper Devonian Horn River Group shale, Northeast British Columbia, Canada. AAPG Bulletin 101: 177–204. https://doi.org/10.1306/07251615199.

Farquhar, R. A., Somerville, J. M., and Smart, B. G. D. 1994. Porosity as a geomechanical indicator: An application of core and log data and rock mechanics. Paper SPE-28853 presented at the European Petroleum Conference, London, United Kingdom. https://doi.org/10.2118/28853-MS.

Gale, J. F. W., Reed, R. M., and Holder, J. 2007. Natural fractures in the Barnett Shale and their importance for hydraulic fracture treatments. AAPG Bulletin 91: 603–622. https://doi.org/10.1306/11010606061.

Gale, J. F. W., Laubach, S. E., Olson, J. E. et al. 2014. Natural fractures in shale: A review and new observations. AAPG Bulletin 98: 2165–2216. https://doi.org/10.1306/08121413151.

Graham, S. A. and Williams, L. A. 1985. Tectonic, depositional, and diagenetic history of the Monterey Formation (Miocene), central San Joaquin basin, California. AAPG Bulletin 69: 385–411.

Gross, M. R. 1995. Fracture partitioning: Failure mode as a function of lithology in the Monterey Formation of coastal California. Geological Society of America Bulletin 107: 779–792. https://doi.org/10.1130/0016-7606%281995%29107%3C0779%3AFPFMAA%3E2.3.CO%3B2.

Güneş Yilmaz, N. G., and Göktan, R. M. 2018. Analysis of the Leeb Hardness Test Data Obtained by Using Two Different Rock Core Holders. Süleyman Demirel Üniversitesi Fen Bilimleri Enstitüsü Dergisi 22 (1): 24. https://doi.org/10.19113/sdufbed.28343.

Holt, R. M., Fjaer, E., Nes, O. M., and Alassi, H. T. 2011. A shaly look at brittleness. Paper ARMA-11-366 presented at the 45th US Rock Mechanics/Geomechanics Symposium, San Francisco, California, USA.

Horsrud, P. 2001. Estimating mechanical properties of shale from empirical correlations. SPE Drilling & Completion 16: 68–73. https://doi.org/10.2118/56017-PA.

Hosford Scheirer, A., ed. 2007. Petroleum systems and geologic assessment of oil and gas in the San Joaquin Basin province, California. US Geological Survey Professional Paper 1713.

Ingle, J. C., Jr. 1981. Cenozoic depositional history of the northern continental borderland of southern California and the origin of associated Miocene diatomites. In Guide to the Monterey Formation in the California Coastal Area, Ventura to San Luis Obispo, ed. C. M. Isaacs, 1–8. Los Angeles, California, USA: Pacific Section, AAPG Special Publication 52.

Ingram, G. M. and Urai, J. L. 1999. Top-seal leakage through faults and fractures: The role of mudrock properties. Geological Society, London, Special Publications 158: 125–135. https://doi.org/10.1144/GSL.SP.1999.158.01.10

Isaacs, C. M. 1980. Diagenesis in the Monterey Formation examined laterally along the coast near Santa Barbara, California. PhD thesis, Stanford University, Stanford, California, USA.

Isaacs, C. M. 1981a. Field characterization of rocks in the Monterey Formation along the coast near Santa Barbara, California. In Guide to the Monterey Formation in the California Coastal Area, Ventura to San Luis Obispo, ed. C. M. Isaacs, 39–54. Los Angeles, California, USA: Pacific Section, Society of Economic Paleontologists and Mineralogists.

Isaacs, C. M. 1981b. Porosity reduction during diagenesis of the Monterey Formation, Santa Barbara coastal area, California. In The Monterey Formation and Related Siliceous Rocks of California, ed. R. E. Garrison and R. G. Douglas, 257–271. Los Angeles, California, USA: Pacific Section, Society of Economic Paleontologists and Mineralogists.

Kahraman, S. 2001. Evaluation of simple methods for assessing the uniaxial compressive strength of rock. International Journal of Rock Mechanics and Mining Sciences 38: 981–994. https://doi.org/10.1016/S1365-1609(01)00039-9.

Keller, M. A. and Isaacs, C. M. 1985. An evaluation of temperature scales for silica diagenesis in diatomaceous sequences including a new approach based on the Miocene Monterey Formation, California. Geo-Marine Letters 5: 31–35. https://doi.org/10.1007/BF02629794.

Kumar, V., Sondergeld, C. H., and Rai, C. S. 2012. Nano to macro mechanical characterization of shale. Paper SPE-159804 presented at the SPE Annual Technical Conference and Exhibition, San Antonio, Texas, USA. https://doi.org/10.2118/159804-MS.

Kuuskraa, V., Stevens, S. H., and Moodhe, K. D. 2013. Technically Recoverable Shale Oil and Shale Gas Resources: An Assessment of 137 Shale Formations in 41 Countries Outside the United States. Washington, DC, USA: US Energy Information Administration and Advanced Resources International (accessed March 2018).

Larue, D. K., Smithard, M., and Mercer, M. 2018. Three deep resource plays in the San Joaquin Valley compared with the Bakken Formation. AAPG Bulletin 102: 195–243. https://doi.org/10.1306/04241716143.

Lashkaripour, G. R. 2002. Predicting mechanical properties of mudrock from index parameters. Bulletin of Engineering Geology and the Environment 61: 73–77. https://doi.org/10.1007/s100640100116.

Lee, J. S. 2015. Calibration of rebound hardness numbers to unconfined compressive strength in shale formations. Journal of Petroleum Technology 67: 41–45. https://doi.org/10.2118/0115-0041-JPT.

Lee, J. S., Smallwood, L., and Morgan, E. 2014. New application of rebound hardness numbers to generate logging of unconfined compressive strength in laminated shale formations. Paper ARMA-2014-6972 presented at the 48th US Rock Mechanics/Geomechanics Symposium, Minneapolis, Minnesota, USA.

Leeb, D. 1979. Dynamic hardness testing of metallic materials. NDT International 12: 274–278. https://doi.org/10.1016/0308-9126(79)90087-7.

Lockman, D. 2012. Monterey Formation opal-A to opal-CT transition core display: Plains Exploration & Production Company, Reardon 330 L North Midway-Sunset field, California. In Monterey Formation Seminar and Core Workshop, AAPG Annual Convention and Exhibition, 103–107. Long Beach, California, USA: AAPG.

Lorenz, J. C., Sterling, J. L., Schechter, D. S., Whigham, C. L., and Jensen, J. L. 2002. Natural fractures in the Spraberry Formation, Midland Basin, Texas: The effects of mechanical stratigraphy on fracture variability and reservoir behavior. AAPG Bulletin 86: 505–524. https://doi.org/10.1306/61EEDB20-173E-11D7-8645000102C1865D.

Miller, D. D. and McPherson, J. G. 1992. South Belridge field — U.S.A., San Joaquin Basin, California. In Structural Traps VII, ed. D. D. Miller and J. G. McPherson, 221–244.

Mohs, F. 1825. Treatise on Mineralogy; Or, the Natural History of the Mineral Kingdom, vol. 1. London, UK: Hurst, Robinson and Company (498 p.).

Mount, V. S. and Suppe, J. 1987. State of stress near the San Andreas fault: Implications for wrench tectonics. Geology 15: 1143–1146.

Mosher, A. 2013. Detailed lithostratigraphic characterization of Chico Martinez Creek, California. MS thesis, California State University, Long Beach, California, USA (115 p.).

Murata, K. J. and Larson, R. R. 1975. Diagenesis of Miocene siliceous shales, Temblor Range, California. Journal of Research of the US Geological Survey 3: 553–566.

Murray, C. D. 2015. Mechanical stratigraphy and sonic log relationships using the Proceq Bambino in the Niobrara Formation, Denver Basin. MS thesis, Colorado School of Mines, Golden, Colorado, USA (88 p.).

Offurum, C. G. 2016. Integrated geochemical, mechanical, and lithological characterization of the Marcellus Shale, Pennsylvania. MS thesis, Texas Christian University, Fort Worth, Texas, USA (125 p.).

Palchik, V. 1999. Influence of porosity and elastic modulus on uniaxial compressive strength in soft brittle porous sandstones. Rock Mechanics and Rock Engineering 32: 303–309. https://doi.org/10.1007/s006030050050.

Palchik, V. and Hatzor, Y. H. 2004. The influence of porosity on tensile and compressive strength of porous chalks. Rock Mechanics and Rock Engineering 37 (4): 331–341.

Passey, Q. R., Bohacs, K., Esch, W. L., Klimentidis, R., and Sinha, S. 2010. From oil-prone source rock to gas-producing shale reservoir—Geologic and petrophysical characterization of unconventional shale gas reservoirs. Paper SPE-131350 presented at the International Oil and Gas Conference and Exhibition in China, Beijing, China. https://doi.org/10.2118/131350-MS.

Peng, J., Milliken, K. L., and Fu, Q. 2020. Quartz types in the Upper Pennsylvanian organic-rich Cline Shale (Wolfcamp D), Midland Basin, Texas: Implications for silica diagenesis, porosity evolution and rock mechanical properties. Sedimentology 67 (4): 2040–2064. https://doi.org/10.1111/sed.12694.

Pisciotto, K. A. 1981. Diagenetic trends in the siliceous facies of the Monterey Shale in the Santa Maria region, California. Sedimentology 28: 547–571. https://doi.org/10.1111/j.1365-3091.1981.tb01701.x.

Pisciotto, K. A. and Garrison, R. E. 1981. Lithofacies and depositional environments of the Monterey Formation, California. In The Monterey Formation and Related Siliceous Rocks of California, ed. R. E. Garrison and R. G. Douglas, 97–122. Los Angeles, California, USA: Pacific Section, Society of Economic Paleontologists and Mineralogists.

Pitman, J. K., Price, L. C., and LeFever, J. A. 2001. Diagenesis and Fracture Development in the Bakken Formation, Williston Basin: Implications for Reservoir Quality in the Middle Member. USGS Professional Paper 1653 (28 p.). Reston, Virginia, USA: US Geological Survey.

Reid, S. A. and McIntyre, J. L. 2001. Monterey Formation porcelanite reservoirs of the Elk Hills field, Kern County, California. *AAPG Bulletin* 85 (1): 169–189. https://doi.org/10.1306/8626C78F-173B-11D7-8645000102C1865D.

Ritz, E., Honarpour, M. M., Dvorkin, J., and Dula, W. F. 2014. Core hardness testing and data integration for unconventionals. Paper URTEC-1916004 presented at the Unconventional Resources Technology Conference, Denver, Colorado, USA. https://doi.org/10.15530/URTEC-2014-1916004.

Ross, D. J. K. and Bustin, R. M. 2008. Characterizing the shale gas resource potential of Devonian–Mississippian strata in the Western Canada sedimentary basin: Application of an integrated formation evaluation. AAPG Bulletin 92: 87–125. https://doi.org/10.1306/09040707048.

Schwalbach, J. R., Gordon, S. A., O'Brien, C. P. et al. 2009. Reservoir characterization of Monterey Formation siliceous shales: Tools and applications. In Contributions to the Geology of the San Joaquin Basin, ed. L. C. Knauer, 119–146. Los Angeles, California, USA: AAPG Pacific Section, MP48.

Schwartz, D. E. 1988. Characterizing the lithology, petrophysical properties, and depositional setting of the Belridge Diatomite, South Belridge field, Kern County, California. In Studies of the Geology of the San Joaquin Basin, ed. S. A. Graham, 281–301. Los Angeles, California, USA: Pacific Section, Society of Economic Paleontologists and Mineralogists, v. 60.

Snyder, W. S., Brueckner, H. K., and Schweickert, R. A. 1983. Deformational styles in the Monterey Formation and other siliceous sedimentary rocks. In Petroleum Generation and Occurrence in the Miocene Monterey Formation, California, ed. C. M. Isaacs and R. E. Garrison, 151–170. Los Angeles, California, USA: Pacific Section, Society of Economic Paleontologists and Mineralogists.

Sonnenfeld, M., Ohlson, C., Zahm, C., and Odegard, M. 2015. The impact of multiple, thin bentonites on proppant placement and effective fracture continuity within the Niobrara Formation, Weld County, Colorado. Paper URTEC-2171548 presented at the Unconventional Resources Technology Conference, San Antonio, Texas, USA. https://doi.org/10.15530/URTEC-2015-2171548.

Tennyson, M. E. and Isaacs, C. M. 2001. Geologic setting and petroleum geology of Santa Maria and Santa Barbara basins, coastal California. In The Monterey Formation—From Rocks to Molecules, ed. C. M. Isaacs and J. Rullkötter, 206–229. New York, USA: Columbia University Press.

Vernik, L., Bruno, M., and Bovberg, C. 1993. Empirical relations between compressive strength and porosity of siliciclastic rocks. International Journal of Rock Mechanics and Mining Sciences & Geomechanics Abstracts 30: 677–680. https://doi.org/10.1016/0148-9062(93)90004-W.

Verwaal, W. and Mulder, A. 1993. Estimating rock strength with the Equotip hardness tester. International Journal of Rock Mechanics and Mining Sciences & Geomechanics Abstracts 30: 659–662. https://doi.org/10.1016/0148-9062(93)91226-9.

Wirtz, Y. and Behl, R. J. 2022. Compositional and diagenetic control of bed- to formational-scale deformation in siliceous sedimentary rocks, Santa Maria Basin, California. In Understanding the Monterey Formation and Similar Biosiliceous Units across Space and Time, ed. Aiello, Barron and Ravello. Geological Society of America Special Publication 556. https://doi.org/10.1130/2022.2556(03).

Yang, S., Harris, N., Dong, T., Wu, W., and Chen, Z. 2015. Mechanical properties and natural fractures in a Horn River Shale core from well logs and hardness measurements. Paper SPE-174287 presented at EUROPEC, Madrid, Spain. https://doi.org/10.2118/174287-MS.

Xiao, N., Chen, J.-Q., Qiu, X., Huang, F., and Ling, T.-H. 2025. Study on the relationship between porosity and mechanical properties based on rock pore structure reconstruction model. Applied Sciences 15 (13): 7247.

Zahm, C. K. and Enderlin, M. 2010. Characterization of rock strength in Cretaceous strata along the Stuart City Trend, Texas. Gulf Coast Association of Geological Societies Transactions 60: 693–702.

Zoback, M. D. 2010. Reservoir Geomechanics. New York, USA: Cambridge University Press (505 p.).